

## Band alignment tuning of InAs quantum dots with a thin AlGaAsSb capping layer

Yu-An Liao, Wei-Ting Hsu, Shih-Han Huang, Pei-Chin Chiu, Jen-Inn Chyi, and Wen-Hao Chang

Citation: *Applied Physics Letters* **102**, 173104 (2013); doi: 10.1063/1.4803013

View online: <http://dx.doi.org/10.1063/1.4803013>

View Table of Contents: <http://scitation.aip.org/content/aip/journal/apl/102/17?ver=pdfcov>

Published by the [AIP Publishing](#)

---

### Articles you may be interested in

[Effects of GaAs\(Sb\) cladding layers on InAs/AlAsSb quantum dots](#)

*Appl. Phys. Lett.* **102**, 023107 (2013); 10.1063/1.4776221

[Observation of band alignment transition in InAs/GaAsSb quantum dots by photoluminescence](#)

*J. Appl. Phys.* **111**, 104302 (2012); 10.1063/1.4717766

[Temperature dependent and time-resolved photoluminescence studies of InAs self-assembled quantum dots with InGaAs strain reducing layer structure](#)

*J. Appl. Phys.* **106**, 013512 (2009); 10.1063/1.3159648

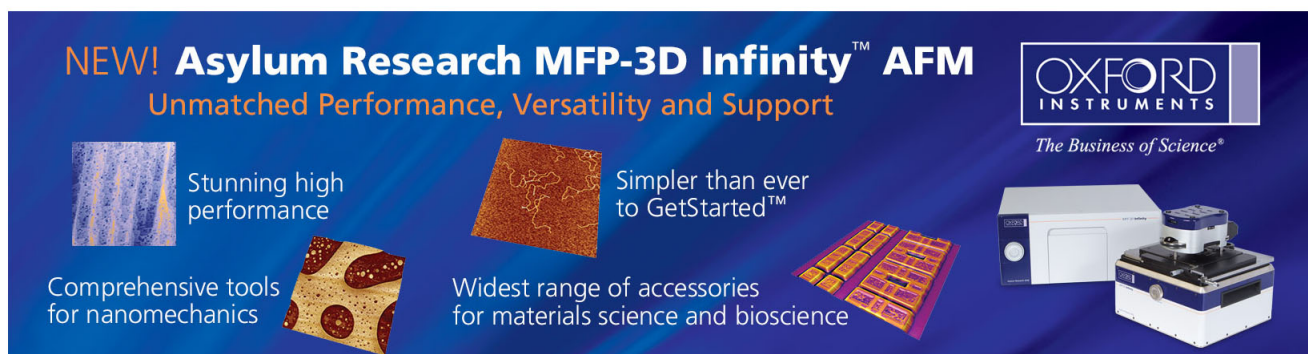
[Thermal peculiarity of AlAs-capped InAs quantum dots in a GaAs matrix](#)

*J. Appl. Phys.* **104**, 104303 (2008); 10.1063/1.3020521

[Effects of a thin InGaAs layer on InAs quantum dots embedded in InAl\(Ga\)As](#)

*Appl. Phys. Lett.* **83**, 3785 (2003); 10.1063/1.1623947

---

The advertisement features a dark blue background with white and orange text. At the top left, it reads 'NEW! Asylum Research MFP-3D Infinity™ AFM' in large white letters, followed by 'Unmatched Performance, Versatility and Support' in orange. On the right, the Oxford Instruments logo is shown with the tagline 'The Business of Science®'. Below the text are four images: a blue textured surface, a brown textured surface, a grid of colorful squares, and a photograph of the AFM instrument. Each image is accompanied by a short text description: 'Stunning high performance', 'Simpler than ever to GetStarted™', 'Comprehensive tools for nanomechanics', and 'Widest range of accessories for materials science and bioscience'.

## Band alignment tuning of InAs quantum dots with a thin AlGaAsSb capping layer

Yu-An Liao,<sup>1,2</sup> Wei-Ting Hsu,<sup>1</sup> Shih-Han Huang,<sup>1</sup> Pei-Chin Chiu,<sup>2</sup> Jen-Inn Chyi,<sup>2</sup> and Wen-Hao Chang<sup>1,a)</sup>

<sup>1</sup>Department of Electrophysics, National Chiao Tung University, Hsinchu 300, Taiwan

<sup>2</sup>Department of Electrical Engineering, National Central University, Zhongli 320, Taiwan

(Received 19 February 2013; accepted 10 April 2013; published online 29 April 2013)

We investigate the optical properties of InAs quantum dots (QDs) capped with a thin  $\text{Al}_x\text{Ga}_{1-x}\text{AsSb}$  layer. As evidenced from power-dependent and time-resolved photoluminescence (PL) measurements, the GaAsSb-capped QDs with type-II band alignment can be changed to type-I by adding Al into the GaAsSb capping layer. The evolution of band alignment with the Al content in the AlGaAsSb capping layer has also been confirmed by theoretical calculations based on 8-band  $\mathbf{k} \cdot \mathbf{p}$  model. The PL thermal stability and the room temperature PL efficiency are also improved by AlGaAsSb capping. We demonstrate that using the quaternary AlGaAsSb can take the advantages of GaAsSb capping layer on the InAs QDs while retaining a type-I band alignment for applications in long-wavelength light emitters. © 2013 AIP Publishing LLC. [<http://dx.doi.org/10.1063/1.4803013>]

Self-assembled InAs quantum dots (QDs) with a GaAsSb capping layer (CL) have attracted much attention recently in the study of improving the performance of long-wavelength QD-based devices.<sup>1–3</sup> The major role of the GaAsSb CL is to reduce the strain inside the QDs, similar to the conventional InGaAs strain reducing layers.<sup>4</sup> The presence of Sb atoms in the CL is also helpful for suppressing the QD decomposition during overgrowth<sup>5,6</sup> and thereby preserving the island height as compared to GaAs-capped QDs. It has been shown that both effects can lead to a redshifted emission wavelength and an improved photoluminescence (PL) efficiency for Sb content less than 12%–14%. As the Sb content exceeds 14%, the InAs-GaAsSb heterointerface becomes a type-II band alignment,<sup>7,8</sup> leading to spatially separated electrons (in the QDs) and holes (in the GaAsSb CL), and resulting in a much longer recombination lifetime.<sup>9,10</sup> Although the type-II InAs/GaAsSb QDs are promising for memory<sup>11</sup> and photovoltaic devices,<sup>12,13</sup> the degraded recombination efficiency is however detrimental for light emitting devices. Several works have been devoted to the tailoring of the optical properties of GaAsSb-capped InAs QDs, such as varying the Sb composition in the GaAsSb CL,<sup>6,7</sup> post-growth thermal treatments,<sup>14,15</sup> varying the GaAsSb CL thickness,<sup>16</sup> graded Sb content in CL,<sup>17</sup> or using quaternary GaAsNSb.<sup>18</sup> However, since the effects of strain reduction and decomposition suppression are proportional to the Sb content in the CL,<sup>6</sup> it seems unlikely to take the advantages of GaAsSb CL while retaining a type-I QD band alignment. In this context, replacing the GaAsSb by an AlGaAsSb CL appears to be a promising alternative. Figure 1(a) shows a contour map of the unstrained valence band offset (VBO) between  $\text{Al}_x\text{Ga}_{1-x}\text{As}_{1-y}\text{Sb}_y$  and InAs [i.e.,  $E_V(\text{Al}_x\text{Ga}_{1-x}\text{As}_{1-y}\text{Sb}_y) - E_V(\text{InAs})$ , where  $E_V$  is the valence band maximum] as functions of the Al ( $x$ ) and the Sb ( $y$ ) contents according to the material parameters in Ref. 19. If the quaternary AlGaAsSb alloy is used for capping the InAs/GaAs QDs, the band alignment can be separated into the type-I and type-II regions by the

boundary of zero VBO (solid line). Although the boundary line would be changed by the inhomogeneous strain distribution and the quantum confinement of the QDs, it is evident that the band alignment can be restored to type I by adding Al into the CL when the Sb content exceeds 0.14. Furthermore, InAs/AlGaAsSb QDs can offer stronger electron confinement when the VBO is zero for certain Al and Sb contents in the CL, which is also preferable for the development of QD-based intermediate-band solar cells.

In this letter, we demonstrate the tuning of band alignment and optical properties of InAs/GaAs QDs using a thin quaternary AlGaAsSb CL. As evidenced from power dependent PL and time-resolved PL (TRPL) measurements, the GaAsSb-capped QDs with type-II band alignment can be changed to type-I by adding Al into the GaAsSb CL. The evolution of band alignment with the Al content in the CL is also compared with theoretical calculations based on 8-band  $\mathbf{k} \cdot \mathbf{p}$  model.

The samples were grown on GaAs substrates by molecular beam epitaxy. After the growth of a 200 nm thick GaAs buffer layer on the substrate, a layer of self-assembled InAs QDs (2.7 monolayers) was deposited at 500 °C and subsequently capped with a 5 nm thick  $\text{Al}_x\text{Ga}_{1-x}\text{As}_{1-y}\text{Sb}_y$  CL. Four samples with nominal Al contents of  $x=0, 0.1, 0.2,$  and  $0.3$  have been grown. The nominal Sb content is  $y=0.2$  for all samples. It is worth to mention that the growth rate for the AlGaAsSb layer in all samples was kept the same (500 nm/h) in order to minimize variations in the Sb incorporation rate and to mitigate Sb segregations. A sample with GaAs capped InAs QDs was also grown as a reference sample of type-I QDs. Finally, all samples were capped by a 50 nm GaAs layer. Atomic force microscopy revealed that uncapped surface QDs are lens shaped, with an average height of 8 nm, an average diameter of 20 nm, and an areal density of about  $3 \times 10^{10} \text{ cm}^{-2}$ . PL was excited by an Ar<sup>+</sup> laser (488 nm), analyzed by a 0.5 m monochromator and detected by an InGaAs photomultiplier tube. TRPL measurements were performed using a 50 ps pulsed laser diode (635 nm/2.5 MHz). The decay traces were recorded using the

<sup>a)</sup>Electronic mail: whchang@mail.nctu.edu.tw

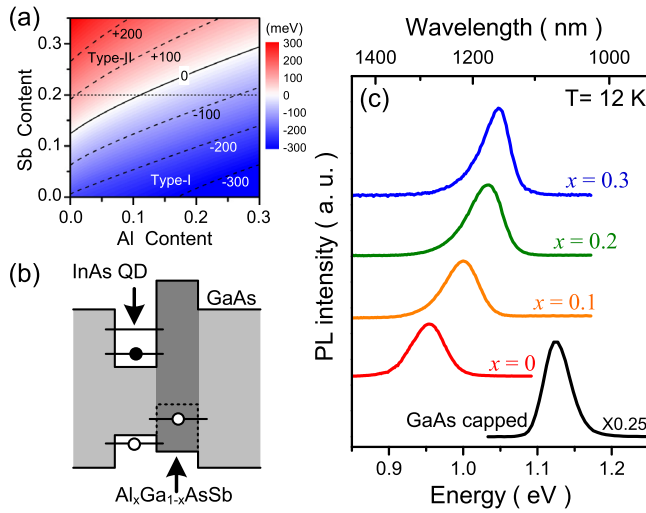


FIG. 1. (a) The contour map of the unstrained VBO between  $\text{Al}_x\text{Ga}_{1-x}\text{As}_{1-y}\text{Sb}_y$  and InAs as functions of the Al ( $x$ ) and the Sb ( $y$ ) contents. (b) A schematic of band alignment for AlGaAsSb-capped InAs/GaAs QDs. (c) The PL spectra measured at  $T = 12$  K for the GaAs-capped and AlGaAsSb-capped InAs QDs with different Al contents ( $x$ ).

time-correlated single photon counting technique with a temporal resolution of  $\sim 150$  ps.

Figure 1(c) shows the PL spectra for the samples measured at  $T = 12$  K under a low excitation power of  $P_{\text{ex}} = 10 \mu\text{W}$ . The QD PL peak blueshifts systematically with increasing Al content  $x$ . For the GaAsSb-capped sample ( $x = 0$ ), the InAs-GaAsSb interface is expected to exhibit a type-II band alignment.<sup>6–8</sup> Since the lattice constant of  $\text{Al}_x\text{Ga}_{1-x}\text{AsSb}$  is similar to that of GaAsSb, strain redistribution caused by adding Al into the CL can be excluded. The blueshift in PL peak can thus be attributed to the reduction in the VBO at the InAs- $\text{Al}_x\text{Ga}_{1-x}\text{AsSb}$  interface.

In order to examine the band alignments, we have performed power dependent PL measurements. Figure 2(a) shows the PL peak energy of QD ground state as a function of the cube root of excitation power  $P_{\text{ex}}^{1/3}$ . The PL peak of GaAsSb-capped QDs shows a large energy blueshift with increasing  $P_{\text{ex}}$  and exhibits a nearly linear dependence on  $P_{\text{ex}}^{1/3}$ , signifying its

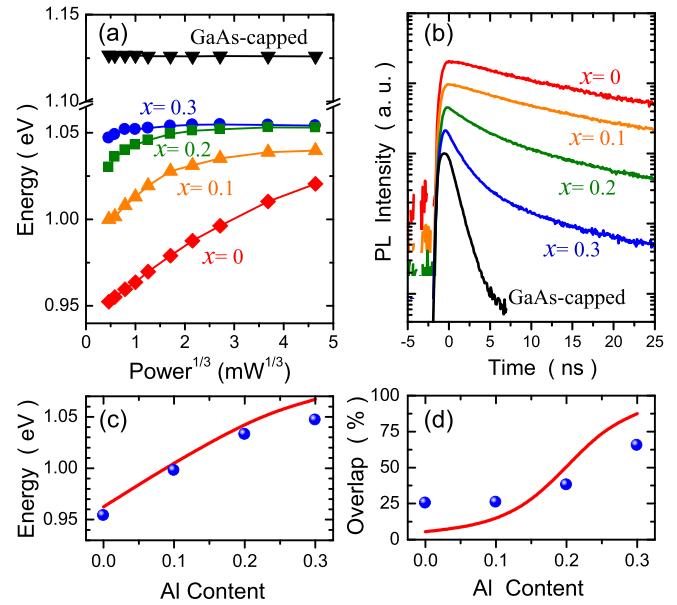


FIG. 2. (a) The ground state PL peak energies as a function of  $P_{\text{ex}}^{1/3}$ . (b) Time-resolved PL spectra for the investigated samples. (c) The ground state PL peak energies as a function of Al contents ( $x$ ). (d) The estimated wave function overlaps according to the measured decay lifetimes.

type-II character.<sup>2,8,10</sup> Such an energy blueshift is not observed in the type-I GaAs-capped QDs. For the AlGaAsSb-capped QDs, the PL peak blueshifts at low excitation powers but becomes nearly unchanged under higher excitation conditions. As the Al content  $x$  in the CL is increased, the energy blueshift becomes less significant. This behavior can be explained by the gradual evolution from type-II to type-I recombination with the increasing Al content  $x$  in the CL. Increasing Al content in the CL tends to reduce the VBO at the QD-CL interface, which becomes unable to confine holes in the CL, resulting in type-I like behaviors. It is remarkable for the AlGaAsSb-capped QDs with  $x = 0.3$ , where the PL peak energy is nearly independent of excitation power, indicating that QD-CL interface has changed to a type-I band alignment.

The QD band alignments can be further investigated by TRPL measurements. Figure 2(b) shows the TRPL decay

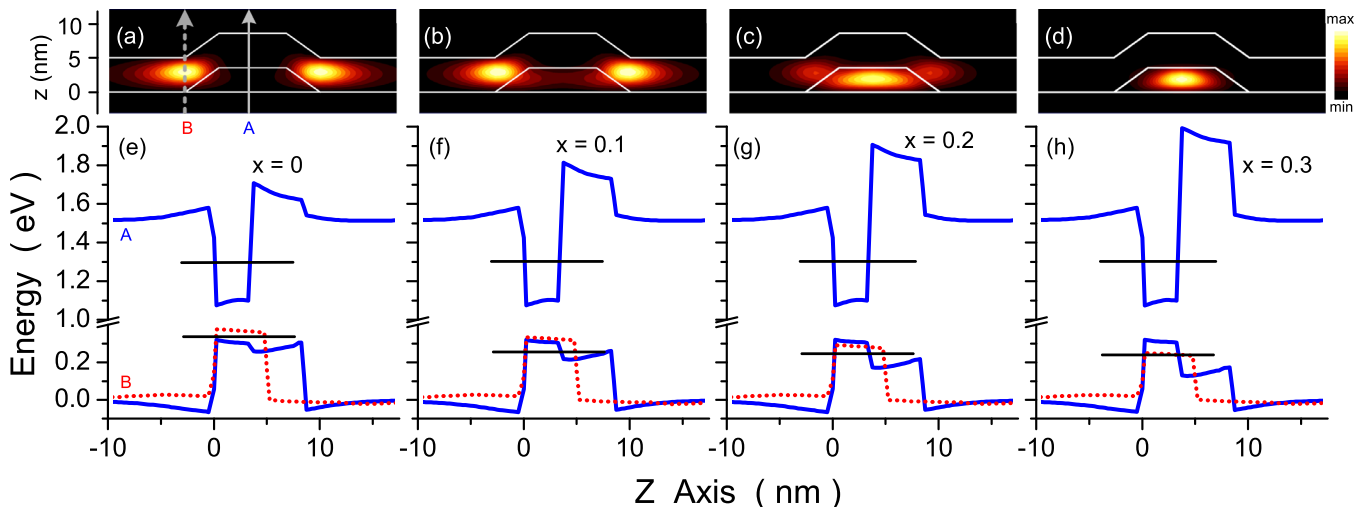


FIG. 3. (a)-(d) The calculated wave function distributions for the hole ground state on the (1–10) plane for different Al contents ( $x = 0, 0.1, 0.2, 0.3$ ) in the CL. (e)-(h) The calculated band structures along the growth direction through the center of the QD (solid line, A) and through the CL near the QD base (dotted line, B).

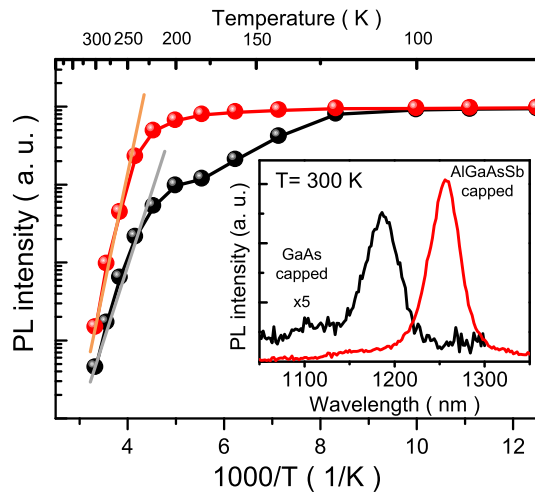


FIG. 4. Arrhenius plot of the integrated PL intensity for GaAs-capped and AlGaAsSb-capped InAs QDs with  $x = 0.3$ . The inset shows the PL spectra measured at room temperature.

traces of the investigated samples measured at  $T = 12$  K. The measured decay lifetime for GaAs-capped QDs in the reference sample is 0.8 ns, comparable to the typical reported value of  $\sim 1$  ns. In contrast, the GaAsSb-capped sample exhibits a much longer lifetime of 15.7 ns due to its type-II band alignment. Increasing Al content in the CL leads to a significant shortening in decay lifetimes, indicating that more hole wave functions penetrate into the QDs. The deduced decay lifetimes are 14.5, 6.5, and 2.2 ns for samples with  $x = 0.1, 0.2,$  and  $0.3$ , respectively. Because the radiative recombination lifetime is inversely proportional to the square of the overlap integral of the electron and hole wave functions and proportional to the emission energy, the measured lifetimes can thus be a measure of the electron-hole overlap in the QDs. If we assume that the overlap in the GaAs-capped type-I QDs is 100%, we estimated that the electron-hole overlaps in the  $\text{Al}_x\text{Ga}_{1-x}\text{As}_{0.8}\text{Sb}_{0.2}$ -capped QDs are 27%, 27%, 40%, and 70% for samples with  $x = 0, 0.1, 0.2,$  and  $0.3$ , respectively.

Theoretical calculations based on eight-band  $\mathbf{k}\cdot\mathbf{p}$  model<sup>20</sup> have been carried out in order to understand the evolution of hole wave function distribution with the Al content  $x$  in the CL. We consider the InAs QD as a truncated pyramid with  $\{101\}$  facets and having a base length  $b = 14$  nm, a height  $h = 3.5$  nm, and a 5 nm  $\text{Al}_x\text{Ga}_{1-x}\text{As}_{0.8}\text{Sb}_{0.2}$  CL covering thereon in a conformal way. The inhomogeneous strain distribution and the strain-induced piezoelectric polarization have also been included. The calculated wave function distributions for the hole ground state on the (110) plane for different Al contents in the CL are depicted in Figs. 3(a)–3(d). For the GaAsSb-capped QDs, the hole wave function is localized in the CL and close to the QD base along the  $[1-10]$  direction, where the potential is a minimum for the hole. With increasing  $x$ , the hole wave function penetrates gradually into the QD and eventually well-localized in the QD for  $x = 0.3$ . This can be attributed to the change of VBO by introducing Al into the CL, as can be seen from the calculated band structures along the growth direction shown in Figs. 3(e)–3(h), where the potential minimum for the hole has been moved from the CL to the QD for  $x \geq 0.2$ . The calculated transition energy and wave

function overlap as function of Al content  $x$  is displayed in Figs. 2(c) and 2(d). They fit very well with the measured PL energy shift and the estimated wave function overlaps. For  $x < 0.1$ , the energy shift rate follows very well with the VBO change rate (4.1 meV/Al%) due to its type-II character. When  $x$  exceeds 0.2, increasing  $x$  only leads to higher confined potentials for both the electron and hole, which have less effect on the transition energy of type-I QDs.

We have also performed temperature-dependent PL measurements in order to understand the thermal stability of QD emission property after AlGaAsSb capping. Figure 4 shows the Arrhenius plot of the integrated PL intensity for GaAs-capped and  $\text{Al}_{0.3}\text{Ga}_{0.7}\text{AsSb}$ -capped InAs QDs. For the conventional GaAs-capped QDs, the PL intensity started to drop at  $T > 120$  K. In contrast, the PL intensity for the  $\text{Al}_{0.3}\text{Ga}_{0.7}\text{AsSb}$ -capped sample can persist up to  $T = 200$  K. The thermal activation energy for PL quenching also increases from 371 to 505 meV, implicating the improved thermal stability of QD PL after AlGaAsSb capping. We would like to mention that the  $\text{Al}_{0.3}\text{Ga}_{0.7}\text{AsSb}$ -capped sample exhibits a large enhancement in the room temperature PL intensity ( $\times 7$ ) as compared with that of the GaAs-capped reference sample. Such an improvement in the optical properties makes the AlGaAsSb capped InAs QDs very promising for long wavelength applications.

In conclusion, the optical properties of AlGaAsSb-capped InAs QDs have been investigated by PL and TRPL measurements. The original type-II band alignment in GaAsSb-capped InAs QDs can be restored to type-I by adding Al into the CL. Furthermore, the AlGaAsSb CL also improves the PL thermal stability and the room temperature PL efficiency. We demonstrate that using a quaternary AlGaAsSb CL can take the advantages of GaAsSb CL (i.e., strain reduction and decomposition suppression) on the InAs QDs while retaining their type-I QD characters.

This work was supported in part by MOE-ATU program and the National Science Council of Taiwan under Grant No. NSC-101-2628-M-009-002-MY3.

- <sup>1</sup>J. M. Ripalda, D. Granados, Y. González, A. M. Sánchez, S. I. Molina, and J. M. García, *Appl. Phys. Lett.* **87**, 202108 (2005).
- <sup>2</sup>H. Y. Liu, M. J. Steer, T. J. Badcock, D. J. Mowbray, M. S. Skolnick, P. Navaretti, K. M. Groom, M. Hopkinson, and R. A. Hogg, *Appl. Phys. Lett.* **86**, 143108 (2005).
- <sup>3</sup>K. Nishikawa, Y. Takeda, K. Yamanaka, T. Motohiro, D. Sato, J. Ota, N. Miyashita, and Y. Okada, *J. Appl. Phys.* **111**, 044325 (2012).
- <sup>4</sup>K. Nishi, H. Saito, S. Sugou, and J.-S. Lee, *Appl. Phys. Lett.* **74**, 1111 (1999); V. M. Ustinov, N. A. Maleev, A. E. Zhukov, A. Yu. Egorov, A. V. Lunev, B. V. Volovik, I. L. Krestnikov, Yu. G. Musikhin, N. A. Bert, P. S. Kop'ev, Zh. I. Alferov, N. N. Ledentsov, and D. Bimberg, *ibid.* **74**, 2815 (1999); N.-T. Yeh, T.-E. Nee, J.-I. Chyi, T. M. Hsu, and C. C. Huang, *ibid.* **76**, 1567 (2000); W.-H. Chang, H.-Y. Chen, H.-S. Chang, W.-Y. Chen, T. M. Hsu, T.-P. Hsieh, J.-I. Chyi, and N.-T. Yeh, *ibid.* **86**, 131917 (2005); P.-C. Chiu, W.-S. Liu, M.-J. Shiau, J.-I. Chyi, W.-Y. Chen, H.-S. Chang, and T.-M. Hsu, *ibid.* **91**, 153106 (2007).
- <sup>5</sup>J. M. Ulloa, I. W. D. Drouzas, P. M. Koenraad, D. J. Mowbray, M. J. Steer, H. Y. Liu, and M. Hopkinson, *Appl. Phys. Lett.* **90**, 213105 (2007).
- <sup>6</sup>J. M. Ulloa, R. Gargallo-Caballero, M. Bozkurt, M. del Moral, A. Guzmán, P. M. Koenraad, and A. Hierro, *Phys. Rev. B* **81**, 165305 (2010).
- <sup>7</sup>H. Y. Liu, M. J. Steer, T. J. Badcock, D. J. Mowbray, M. S. Skolnick, F. Suarez, J. S. Ng, M. Hopkinson, and J. P. R. David, *J. Appl. Phys.* **99**, 046104 (2006).
- <sup>8</sup>C. Y. Jin, H. Y. Liu, S. Y. Zhang, Q. Jiang, S. L. Liew, M. Hopkinson, T. J. Badcock, E. Nabavi, and D. J. Mowbray, *Appl. Phys. Lett.* **91**, 021102 (2007).

- <sup>9</sup>Y. D. Jang, T. J. Badcock, D. J. Mowbray, M. S. Skolnick, J. Park, D. Lee, H. Y. Liu, M. J. Steer, and M. Hopkinson, *Appl. Phys. Lett.* **92**, 251905 (2008).
- <sup>10</sup>W.-H. Chang, Y.-A. Liao, W.-T. Hsu, M.-C. Lee, P.-C. Chiu, and J.-I. Chyi, *Appl. Phys. Lett.* **93**, 033107 (2008).
- <sup>11</sup>A. Marent, M. Geller, A. Schliwa, D. Feise, K. Pötschke, D. Bimberg, N. Akçay, and N. Öncan, *Appl. Phys. Lett.* **91**, 242109 (2007).
- <sup>12</sup>R. B. Laghumavarapu, A. Moscho, A. Khoshaklagh, M. El-Emawy, L. F. Lester, and D. L. Huffaker, *Appl. Phys. Lett.* **90**, 173125 (2007).
- <sup>13</sup>W.-S. Liu, H.-M. Wu, F.-H. Tsao, T.-L. Hsu, and J.-I. Chyi, *Sol. Energy Mater. Sol. Cells* **105**, 237 (2012).
- <sup>14</sup>Y.-A. Liao, W.-T. Hsu, P.-C. Chiu, J.-I. Chyi, and W.-H. Chang, *Appl. Phys. Lett.* **94**, 053101 (2009).
- <sup>15</sup>J. M. Ulloa, J. M. Llorens, B. Alén, D. F. Reyes, D. L. Sales, D. González, and A. Hierro, *Appl. Phys. Lett.* **101**, 253112 (2012).
- <sup>16</sup>W.-T. Hsu, Y.-A. Liao, F.-C. Hsu, P.-C. Chiu, J.-I. Chyi, and W.-H. Chang, *Appl. Phys. Lett.* **99**, 073108 (2011).
- <sup>17</sup>A. Hospodková, M. Zíková, J. Pangrác, J. Oswald, K. Kuldová, J. Vyskočil, and E. Hulicius, *J. Cryst. Growth* **370**, 303 (2013).
- <sup>18</sup>J. M. Ulloa, D. F. Reyes, M. Montes, K. Yamamoto, D. L. Sales, D. Gonzalez, A. Guzman, and A. Hierro, *Appl. Phys. Lett.* **100**, 013107 (2012).
- <sup>19</sup>I. Vurgaftman, J. R. Meyer, and L. R. Ram-Mohan, *J. Appl. Phys.* **89**, 5815 (2001).
- <sup>20</sup>Numerical calculations were performed using the nextnano<sup>3</sup> 3D nanodevice simulator.